ISSN 1063-7834, Physics of the Solid State, 2020, Vol. 62, No. 6, pp. 942–946. © Pleiades Publishing, Ltd., 2020.
Russian Text © The Author(s), 2020, published in Fizika Tverdogo Tela, 2020, Vol. 62, No. 6, pp. 834–838.

SEMICONDUCTORS

# Electric and Galvanomagnetic Properties of $Cd_3As_2$–20 mol % MnAs Composite under High Pressure

**L. A. Saypulaeva[a, *], M. M. Gadzhialiev[a], A. G. Alibekov[a], N. V. Melnikova[b], V. S. Zakhvalinskii[c], A. I. Ril'[d], S. F. Marenkin[d], and A. N. Babushkin[b]**

[a] *Amirkhanov Institute of Physics, Dagestan Scientific Center, Russian Academy of Sciences, Makhachkala, Russia*
[b] *Ural Federal University, Institute of Natural Sciences and Mathematics, Yekaterinburg, Russia*
[c] *Belgorod National Research University, Belgorod, Russia*
[d] *Kurnakov Institute of General and Inorganic Chemistry, Russian, Academy of Sciences, Moscow, Russia*
**e-mail: luizasa11@mail.ru*

Received December 30, 2019; revised December 30, 2019; accepted January 10, 2020

**Abstract**—The pressure dependences of electrical resistance, Hall coefficient, charge carrier mobilities, and magnetoresistance of the $Cd_3As_2$–20 mol % MnAs composite are investigated at pressures up to 9 GPa. The pressure dependences of all the listed properties exhibit features related to phase transitions. The presence of pressure-induced negative magnetoresistance is registered.

**Keywords:** high pressure, Hall effect, electrical resistivity, negative magnetoresistance, structural phase transition

**DOI:** 10.1134/S1063783420060256

## 1. INTRODUCTION

The compound $Cd_3As_2$ is a Dirac semimetal—a special class of topological insulators—and a three-dimensional graphene analogue [1]. In these materials, charge carriers are represented by Dirac fermions with zero effective mass and subject to relativistic laws of motion. The material features an unusually high electron mobility considerably exceeding $10^4$ cm$^2$/(V s) at room temperature and $10^6$ cm$^2$/(V s) at low temperatures [1]. $Cd_3As_2$ has garnered research interest due to a number of special properties, e.g., nontrivial band structure and highly mobile electrons, and its promising use in different areas of technology. To manipulate the spin ensemble of highly mobile charge carriers in $Cd_3As_2$, we must create topological insulators that allow controllably incorporate, in their crystal lattice, atoms with uncompensated intrinsic magnetic moment (Fe, Mn, V, Cr, and Co). If $Cd_3As_2$ is chosen to represent a Dirac semimetal, then, in order to reduce the formation of extra phases during synthesis, we must select a ferromagnetic material among the compounds consisting of a magnetic atom and As. In this respect, the Mn–As system is considered to be the most known. No stable chemical compounds were identified in this system at a low Mn content (<50 mol %). For this reason, the Mn–As system with a Mn content in excess of 50 mol % was used in synthesis of $Cd_3As_2$–MnAs composites [2].

Manganese dissolves in $Cd_3As_2$ to give a broad region of $(Cd_{1-x}Mn_x)_3As_2$ ternary solid solutions. At high manganese concentrations, a $Cd_3As_2$-based composite is formed, which contains MnAs inclusions along with the $(Cd_{1-x}Mn_x)_3As_2$ solid solution [2]. So far, the physical properties of $Cd_3As_2$–MnAs composites have not been fully investigated.

The aim of this work is to investigate the effects that pressure, temperature, and magnetic field have on the electrical and galvanomagnetic properties (the Hall effect and magnetoresistance) of the $Cd_3As_2$–20 mol % MnAs composite.

Considering the formulated aim, we must address the following problems: (i) to investigate the effect that hydrostatic pressure up to 9 GPa in a magnetic field up to 5 kOe have on the electrical resistance, magnetoresistance, the Hall coefficient, and the charge carrier mobility; and (ii) to study the temperature dependences of the electrical parameters in the temperature range of 77–450 K.

## 2. EXPERIMENTAL TECHNIQUES AND EQUIPMENT

Bulk $Cd_3As_2$–MnAs samples were synthesized in the Kurnakov Institute of General and Inorganic Chemistry (IGIC), Russian Academy of Sciences (RAS) [2]. The alloy was synthesized using $Cd_3As_2$ and MnAs in evacuated ampoules at the temperature

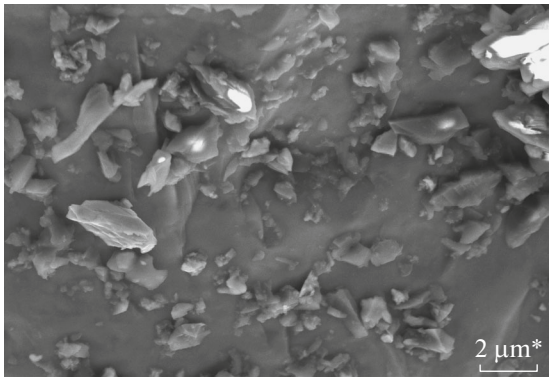


**Fig. 1.** Topographical SEM image of a $Cd_3As_2$–20 mol % MnAs sample.

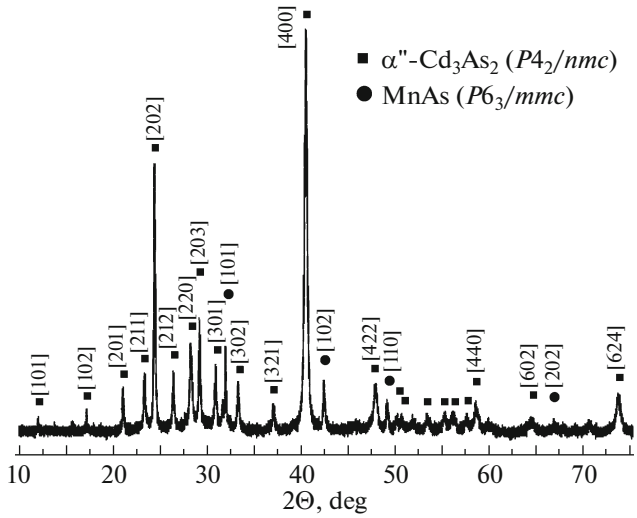


**Fig. 2.** XRD pattern of the synthesized sample.

of manganese arsenide melting point. The structure, composition, and surface element distribution of prepared samples were studies using JSM-6610LV (JEOL) scanning electron microscope (SEM) equipped with an X-MaxN attachment for energy-dispersive X-ray analysis (Oxford Instruments).

Electron microscopy study of a cross section of the $Cd_3As_2$–20 mol % MnAs sample identified that the sample was not single-crystal and consists of large crystal blocks (Fig. 1).

The phase composition of the sample was identified by X-ray powder diffraction (XRD) on a BRUKER D8 ADVANCE X-ray diffractometer (facilities of the Center of Collective Use, IGIC, RAS) using Cu$K_\alpha$ radiation. XRD patterns were recorded at a step of 0.014° with holding time of 1.3 s. The ICDD PDF-2 database for powder diffraction data and the Diffrac.SuiteEVA software were used. In addition, sample characterization was performed using an instrument for differential thermal analysis (DTA) built in IGIC, RAS.

Two key phases were identified on the XRD patterns (Fig. 2): the tetragonal $Cd_3As_2$ and hexagonal (ferromagnetic) MnAs. Also, the presence of small quantities of the $CdAs_2$ phase was detected.

High hydrostatic pressures, up to 9 GPa, were achieving using a toroid-type cell [3, 4]. Samples were solid blocks with dimensions 3 × 1.0 × 1.0 mm.

Hall coefficient $R_H$ was measured by applying direct current $I$ in a stationary magnetic field $H$. $R_H$ depends on the electron and hole concentration and mobility. If free electrons is the only charge carrier in a given material, we have $R_H = 1/ne$, where $n$ is the electron concentration and $e$ is the electron charge.

## 3. RESULTS AND DISCUSSION

The electrical properties of the structures under study depend on the granule size and packing density. If the average particle density in a material is small, its conductivity is accordingly quite low. At a higher density, i.e., when a considerable number of particles are in contact with one another, quite extended clusters may form in the structure, and the conductivity of the structure will exhibit a more complex pattern than in cases when the additivity rule applies. The actual conductivity of the composite is determined by both the conductivity of MnAs and $Cd_3As_2$ phases, the conductivity of a transition layer between them, and the granule shape. The tunneling probability of charge carriers depends on the size and distance between granules; the height, width, and shape of tunneling barriers; and the temperature of medium.

The temperature dependent resistivity $\rho(T)$ of the $Cd_3As_2$–20 mol % MnAs composite in the temperature range of 77–450 K is shown in Fig. 3. The composite exhibits metallic conductivity in the studied temperature range. A sharp rise in the resistivity in the temperature range of 300–330 K (Fig. 3) reflects a change in the mechanism of scattering of conductivity electrons at the boundaries between nonmagnetic and MnAs regions in the composite that, in this temperature range, changed from being ferromagnetic to paramagnetic (the Curie point for MnAs is ~318 K [5]).

Pressure dependences of the resistivity (registered both on raising and lowering the pressure), the Hall coefficient, and magnetoresistance at different applied magnetic fields are shown in Fig. 4. As the pressure is raised to 2.8 GPa (Fig. 4a), the electrical resistivity increases very gradually and monotonically until it exhibits a drastic rise, and the rate of this rise (i.e., the derivative $\partial\rho/\partial P$) attains a maximum at $P = 4.2$ GPa, which is followed by a more gradual rise. As the pressure is lowered, the resistivity changes nonmonotonically: it falls, having different pressure coefficients and reaches a maximum is at $P = 2.75$ GPa. The pressure

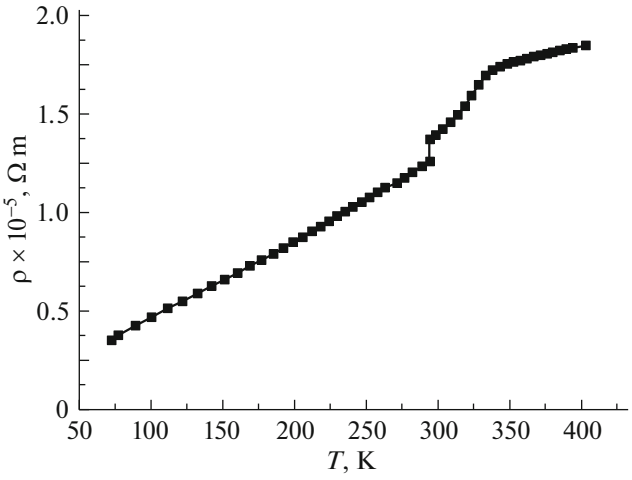


**Fig. 3.** Temperature-dependent electrical resistivity.

dependences of electrical resistivity in the pressure range of 15 to 50 GPa can be found elsewhere [6].

Assuming that the electrical and magnetic properties at atmospheric pressure are mainly dictated by the behavior of MnAs nanoclusters, as is the case with $Cd_3As_2$–MnAs composite (52.7 at % MnAs) [6], changes in the distance between granules, along with possible manifestations of structural characteristics and properties of the matrix, become an important factor at high pressures.

Hall coefficient $R_H$ has a maximum at pressure $P \approx 3.65$ GPa and exhibits a pattern correlating to pressure dependence $\rho(P)$.

The pressure dependences of Hall mobility for the $Cd_3As_2$–20 mol % MnAs composite are shown in Fig. 4b. The most rapid decline in the mobility with the increasing pressure is observed in the range of 3.3 to 4.2 GPa.

The presence of negative magnetoresistance (nMR) with a maximum (~1%) in the range of 1–2.6 GPa can be seen on the pressure dependences shown in Fig. 4c. Features of positive magnetoresistance are conspicuously expressed in the material under study, along with the presence of nMR (Fig. 4c): the maximum that occurs on the pressure dependences of magnetoresistance at around 4 GPa grows with the increasing magnetic field strength. We studied field dependences of magnetoresistance at

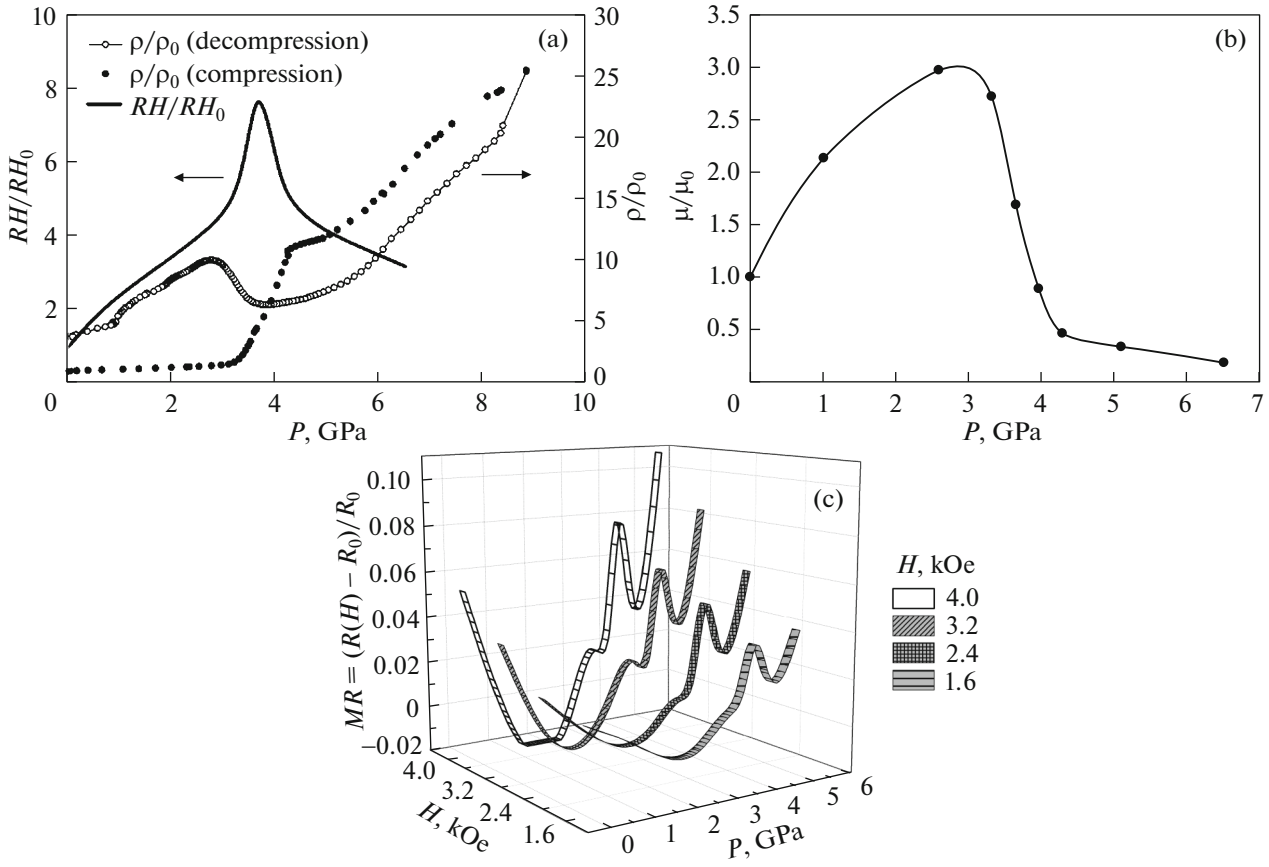


**Fig. 4.** Pressure dependences of (a) electrical resistivity registered on rising and lowering the pressure and the Hall coefficient, (b) charge carrier mobilities, and (c) magnetoresistance at different strengths of applied magnetic field.

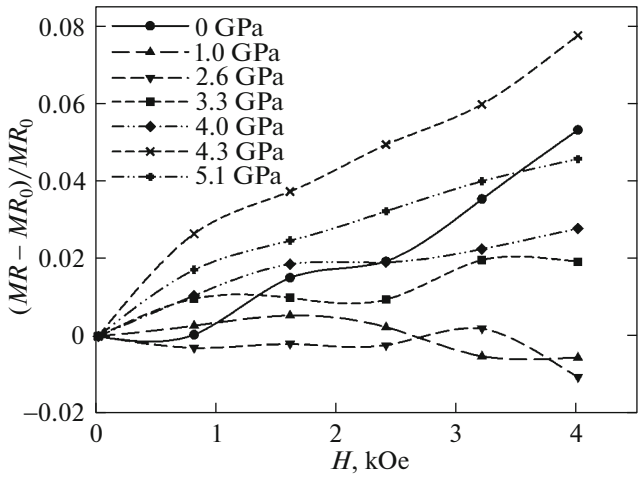


**Fig. 5.** Field dependence of magnetoresistance at different pressures.

fixed pressure values in order to better identify the conditions for manifestation of nMR (Fig. 5).

Thus, in the presented pressure dependences of electrical resistance, Hall coefficient, charge carrier mobilities, and magnetoresistance at 3–4 GPa, we identified the specific features corresponding to phase transitions in the semiconducting matrix of the $Cd_3As_2$ composite and in its ferromagnetic MnAs granules. It is reasonable to assume that applying a high pressure results in an overlap of phase transitions in the $Cd_3As_2$–20 mol % MnAs alloy, which is a structural phase transition in the $Cd_3As_2$ matrix.

The transformation of the tetragonal structure to a monoclinic one occurs in the pressure range of 2.6–4.0 GPa, which supports previous findings [7]. Neutron diffraction studies of the MnAs atomic and magnetic structures at pressures up to 38 bar and in the temperature range of 15–300 K [8] showed that in MnAs the spin reorientation transition from the orthorhombic phase into a new phase occurs at high pressures as the temperature is lowered, with the magnetic moment of the new phase having both ferromagnetic and antiferromagnetic components.

The causes of nMR in semiconductors and mechanisms of nMR emergence in granular structures, in particular, in $Cd_3As_2$–MnAs alloys were reported and discussed in a series of studies [9–13].

Under high pressures, the distance between MnAs granules shorten and the features of structural characteristics and properties of the $Cd_3As_2$ matrix change. Carrier transport properties in granular structures are determined not only by transfer processes in granules, but also carrier tunneling between granules. If the size of granules is comparable to that of magnetic domains, the magnetic moments of granules are aligned parallel to the applied magnetic field, which leads to lesser scattering of conductivity electrons and emergence of nMR. While the strength of externally applied magnetic field is increased, causing ordering in the magnetization of individual magnetic moments, the tunneling resistance decreases. As the pressure is raised, the tunneling resistance falls due to shortening the distance between granules, i.e., due to reducing the tunneling barrier height. Moreover, we must also take into account the presence of electrically active defects in the matrix that emerged during the synthesis of composite material and the formation of MnAs granules that can be a source of electrons or holes. A fraction of defects represents uncompensated atoms with a nonzero spin that can function as localized magnetic moments or magnetic sites for charge scattering when a magnetic field is applied.

Assuming that the size of ferromagnetic granules in $Cd_3As_2$–20 mol % MnAs is much smaller than in $Cd_3As_2$–44.7 mol % MnAs [14]—since SEM characterization of the former material did not reveal the presence of granules in it—we can expect that such an ensemble will respond to an applied magnetic field at lower pressures. In this case, the total surface area of nanogranules that mediate the supply of a fraction of conductivity electrons into the $Cd_3As_2$ matrix increases, and when the material is exposed to a progressively higher pressure, the matrix undergoes deformation, its electrical resistance decreases, and the distance between granules shortens; while in an applied magnetic field the nanogranule magnetic moments are aligned parallel to the field even at moderate pressures.

## 4. CONCLUSIONS

The effect of high pressure on the electrical and galvanomagnetic properties of the $Cd_3As_2$–20 mol % MnAs composite is studied. In the pressure region of 3–4 GPa, the registered pressure dependences of electrical resistance, Hall coefficient, charge carrier mobilities, and magnetoresistance exhibit features related to phase transitions in the semiconducting matrix of $Cd_3As_2$ composite and in its MnAs ferromagnetic granules. The pressure dependences of magnetoresistance exhibit an nMR feature that reaches a maximum (around 1%) in the pressure range of 1–2.6 GPa. In addition to the presence of nMR, the material under study displays conspicuous features of positive magnetoresistance: the height of a peak observed around 4 GPa on the pressure-dependent magnetoresistance curve increases with increasing the strength of the applied magnetic field.

## CONFLICT OF INTEREST

The authors declare that they have no conflicts of interest.

## REFERENCES


1. T. Liang, Q. Gibson, M. N. Ali, M. Liu, R. J. Cava, and N. P. Ong, Nat. Mater. **14**, 280 (2015).
2. A. I. Ril', A. V. Kochura, S. F. Marenkin. A. E. Kukz'ko, and B. A. Aronzon, Izv. Yu.-Zap. Univ., Ser. Tekh. Tekhnol. **7** (2), 120 (2017).
3. L. G. Khvostantsev, L. P. Vereshchagin, and A. P. Novikov, High Temp.-High Press. **9**, 637 (1977).
4. A. Yu. Mollaev, L. A. Saipulaeva, R. K. Arslanov, and S. F. Marenkin, Inorg. Mater. **37**, 327 (2001).
5. N. P. Grazhdankina, Sov. Phys. Usp. **11**, 727 (1968).
6. N. V. Melnikova, A. V. Tebenkov, G. V. Sukhanova, A. N. Babushkin, L. A. Saipulaeva, V. S. Zakhavalinskii, S. F. Gabibov, A. G. Alibekov, and A. Yu. Mollaev, Solid State Phys. **60**, 499 (2018).
7. L. He, Y. Jia, S. Zhang, X. Hong, C. Jin, and S. Li, npj Quantum Mater. 1, 16014 (2016).
8. V. P. Glazkov, D. P. Kozlenko, K. M. Podurets, B. N. Savenko, and V. A. Somenkov, Crystallogr. Rep. **48**, 54 (2003).
9. I. V. Bondar', S. V. Trukhanov, and T. H. Barugu, Semiconductors **49**, 1276 (2015).
10. Yu. V. Kabirov, V. G. Gavrilyachenko, A. S. Bogatin, N. V. Lyanguzov, T. V. Gavrilyachenko, and A. A. Klenushkin, Phys. Solid State **58**, 1304 (2016).
11. S. F. Marenkin, A. D. Izotov, I. V. Fedorchenko, and V. M. Novotortsev, Russ. J. Inorg. Chem. **60**, 295 (2015).
12. X. L. Wang, Q. Shao, and A. Zhuravlyova, Sci. Rep. **5**, 9221 (2015).
13. A. G. Alibekov, A. Yu. Mollaev, L. A. Saipullaeva, S. F. Marenkin, and I. V. Fedorchenko, Inorg. Mater. **52**, 357 (2016).
14. L. A. Saipulaeva, Sh. B. Abdulvagidov, M. M. Gadzhialiev, A. G. Alibekov, N. V. Mel'nikova, E. A. Stepanova, D. O. Alikin, V. S. Zakhvalinskii, A. I. Ril', S. F. Marenkin, and Z. Sh. Pirmagomedov, Fiz. Tekh. Vys. Davl. **29** (4), 48 (2019).


*Translated by A. Kukharuk*